Biochimica et Biophysica Acta 1850 (2015) 318–328

Contents lists available at ScienceDirect

Biochimica et Biophysica Acta

journal homepage: www.elsevier.com/locate/bbagen

Evidence for the requirement of CydX in function but not assembly of the cytochrome *bd* oxidase in *Shewanella oneidensis*

Haijiang Chen [1], Qixia Luo [1], Jianhua Yin, Tong Gao, Haichun Gao *

Institute of Microbiology and College of Life Sciences, Zhejiang University, Hangzhou, Zhejiang 310058, China

ARTICLE INFO

Article history:
Received 11 July 2014
Received in revised form 25 September 2014
Accepted 6 October 2014
Available online 12 October 2014

Keywords:
Shewanella
bd oxidase
CydX

ABSTRACT

Background: Cytochrome *bd* oxidase, existing widely in bacteria, produces a proton motive force by the vectorial charge transfer of protons and more importantly, endows bacteria with a number of vitally important physiological functions, such as enhancing tolerance to various stresses. Although extensively studied as a CydA–CydB two-subunit complex for decades, the complex in certain groups of bacteria is recently found to in fact consist of an additional subunit, which is functionally essential.
Methods: We investigated the assembly of the CydA–CydB complex using BiFC. We investigated the function of CydX using mutational analysis.
Results: CydX, a 38-amino-acid inner-membrane protein, is associated with the CydA–CydB complex in *Shewanella oneidensis*, a facultative anaerobe renowned for its respiratory versatility. It is clear that CydX is neither required for the *in vivo* assembly of the CydA–CydB complex nor relies on the complex for its translocation and integration into the membrane. The N-terminal segment (1–25 amino acid residues) and short periplasmic overhang of CydX, with respect to functionality, are important whereas the remaining C-terminal segment is rather flexible.
Conclusion: Based on these findings, we postulate that CydX may function by positioning and stabilizing the prosthetic hemes, especially heme *d* in the CydA–CydB complex although a role of participating in catalytic reaction is not excluded.
General significance: The work provides novel insights into our understanding of the small subunit of the cytochrome *bd* oxidase.

1. Introduction

Cytochrome *bd* respiratory oxidase is found in a wide variety of prokaryotes, especially pathogens [1–3]. The terminal oxidase is well-known for its extremely high affinity to molecular oxygen consistent with its high expression and functioning in micro-aerobic conditions [4]. In addition, the enzyme is involved in protective mechanisms against various stresses, most of which are elicited by the host [5–10]. For these reasons, cytochrome *bd* oxidase is indispensable for some pathogens when they are infecting the host tissues which can be considered as micro-aerobic environments [11]. Furthermore, cytochrome *bd* oxidase confers bacteria the ability to tolerate dozens of respiration inhibitors which bind more readily to and thus outcompete binding of oxygen to heme-copper oxygen reductase, a different type of terminal oxidase universally existing in cellular organisms [1,12].

Shewanella are Gram-negative facultative-anaerobes predominantly residing in redox-stratified environments, which compel this group of microorganisms to accommodate different O_2 concentrations and use a variety of electron acceptors when O_2 is depleted [13]. To facilitate the adaptation, *Shewanella* have evolved multiple terminal cytochrome enzymes, including cytochrome caa_3- and cbb_3-type heme-copper oxidases (HCOs) and a cytochrome *bd* oxidase, as illustrated in research model *Shewanella oneidensis*[14]. In prior work we have shown that the cbb_3 oxidase is the predominant system for respiration of oxygen whereas the caa_3 oxidase, an analogue to the mitochondrial enzyme, has no physiological significance [15,16]. Although the cytochrome *bd* oxidase has a significant role in addition to the cytochrome cbb_3 oxidase under microaerobic conditions, its major contribution to the cell is to facilitate adaptation to a variety of stress conditions [16–18]. In particular, the *bd* oxidase confers nitrite resistance to *S. oneidensis* during aerobic growth [17].

It is a long held view that the cytochrome *bd* oxidase consists of two subunits, CydA and CydB [1]. In *Escherichia coli*, there are two gene clusters coding cytochrome *bd* oxidase, namely *cydAB* and *cyxAB* (*appCB*, or *cbdAB*) and deletion of each one can be functionally compensated by the other [19]. However, about 17 years ago a small ORF (mostly named *ybgT*) immediately downstream the coding genes for CydAB was identified in *E. coli*[20]. The ORF, encoding a small protein of the YbgT–YccB superfamily, is conserved across the Proteobacteria,

* Corresponding author.
E-mail address: haichung@zju.edu.cn (H. Gao).
[1] These authors contributed equally to this work.

http://dx.doi.org/10.1016/j.bbagen.2014.10.005
0304-4165/

suggesting a functional involvement of the small protein in the oxidase complex [21–23]. Moreover, the temporal and physiological condition of *ybgT* expression is in accordance with that of *cydAB*[21]. Recently, direct evidence is reported. In intracellular pathogen *Brucella abortus*, this small protein, renamed as CydX, has been demonstrated to be required for the function of the cytochrome *bd* oxidase [24]. In *E. coli*, CydX is found to be co-purified with either CydA and CydB and essential to proper functioning of *bd*-I terminal oxidase [25].

Despite these progresses, we still know little about how this small protein works. Is it a chaperon required for the assembly of *bd* oxidases or a subunit of the enzyme complex for activity? In a continuous effort to improve the understanding of the *S. oneidensis* cytochrome *bd* oxidase, we further our investigation into CydX to address these questions. We present evidence to suggest that the CydX subunit, in contrast to those characterized recently, is not absolutely essential to the oxidase activity. In addition, complexation of the CydA and CydB subunits is independent of CydX, suggesting that CydX is unlikely to function as a chaperon. Furthermore, both periplasmic and transmembrane segments are important for the functionality of CydX in *S. oneidensis*.

2. Materials and methods

2.1. Strains, plasmids, PCR primers and culture condition

A list of all bacterial strains and plasmids used in this study is given in Table 1. All primers were synthesized by Sangon Biotech (Shanghai) and listed in Table S1. *E. coli* and *S. oneidensis* strains were grown in Luria–Bertani medium at 37 and 30 °C for genetic manipulation, respectively. Where needed, antibiotics were added at the following concentrations: ampicillin at 50 μg/ml, kanamycin at 50 μg/ml, and gentamycin at 15 μg/ml.

2.2. Mutagenesis and in trans complementation

In-frame deletion strains derived from *S. oneidensis* MR-1 were constructed by the *att*-based Fusion PCR method as previously described [26]. For *in trans* complementation of the resulting mutants, vectors pHG101 and pHG102 were utilized [27]. For complementation of genes next to their promoter, a fragment containing the gene of interest and its native promoter was generated by PCR and cloned into pHG101. For the remaining genes, the gene of interest was amplified and inserted into the MCS of pHG102 under the control of the *arcA* promoter, which is constitutively active [28]. For $yneM_{EC}$, $acrZ_{EC}$, Y_N-C_C, and C_N-A_C genes, oligos were synthesized and cloned into pHG102. The resulting complementation vector was transferred into its corresponding mutant strain *via* conjugation and its presence was confirmed by plasmid purification and restriction enzyme digestion.

2.3. Physiological characterization

For phenotypic growth assay, fresh LB media were inoculated with overnight culture to ~0.01 of the optical density at 600 nm (OD_{600}) and shaken on a rotary platform (250 rpm). Readings of OD_{600} were recorded every hour after initial inoculation. For examination of nitrite sensitivity, cells of mid-log phase were adjusted to approximately 10^8 cfu/ml with fresh LB, followed by 10-fold serial dilutions. 5 μl of

Table 1
Strains and plasmids used in this study.

Strain or plasmid	Description	Reference or source
E. coli strains		
MG1655	Wild type	Lab stock
WM3064	Donor strain for conjugation; Δ*dapA*	W. Metcalf, UIUC
S. oneidensis strains		
MR-1	Wild-type	ATCC 700550
HGPCYD	ΔP*cyd* derived from MR-1, lacking the *cyd* promoter	This study
HG0837	Δ*blaA* derived from MR-1	[38]
HGCYD	Δ*cyd* derived from MR-1, lacking the entire *cydABX* operon	This study
HG3284	Δ*cydX* derived from MR-1	This study
HG3285	Δ*cydB* derived from MR-1	[17]
HG3286	Δ*cydA* derived from MR-1	This study
HG3286-5	Δ*cydAB* derived from MR-1	This study
Plasmids		
pHGM01	Ap^R, Gm^R, CM^R, suicide vector	[26]
pHG101	Promoterless vector for complementation	[27]
pHG102	P_{ArcA} vector for complementation	[27]
pHGE-P*tac*	IPTG inducible expression vector containing P*tac* promoter	[32]
pHG101-*cydAB*	pHG101 containing *cydAB*	This study
pHG101-*cydAB*-GFP	pHG101 containing *cydAB* and the GFP gene	This study
pHG102-*cydX*	pHG102 containing *cydX*	This study
pHG102-$cydX_{EC}$	pHG102 containing *E. coli cydX*	This study
pHG102-$yccB_{EC}$	pHG102 containing *E. coli yccB*	This study
pHG102-GFP	pHG102 expressing GFP protein	This study
pHG102-BlaA-*cydX*	pHG102 expressing BlaA-CydX fusion protein	This study
pHG102-*cydX*-BlaA	pHG102 expressing CydX-BlaA fusion protein	This study
pHG102-GFP-*cydX*	pHG102 expressing GFP-CydX fusion protein	This study
pHG102-*cydX*-GFP	pHG102 expressing CydX-GFP fusion protein	This study
pHG102-Y_N-C_C	pHG102 expressing fused protein of *E. coli* YneM (1–25 a.a.) and CydX (25–38 a.a)	This study
pHG102-C_N-A_C	pHG102 expressing fused protein of CydX (1–24 a.a) and *E. coli* AcrZ (30–49 a.a.)	This study
pHG102-Peri	pHG102 expressing fused protein of *E. coli* YneM (1–6 a.a.) and CydX (7–38 a.a)	This study
pHGE-DP*tac*	IPTG inducible expression vector containing two P*tac* promoters in tandem	This study
pHGE-TatA-YFP_N	pHGE-P*tac* expressing TatA-YFP_N	This study
pHGE-TatA-YFP_C	pHGE-P*tac* expressing TatA-YFP_C	This study
pHGE-CydA-YFP_N	pHGE-P*tac* expressing CydA-YFP_N	This study
pHGE-CydB-YFP_C	pHGE-P*tac* expressing CydB-YFP_C	This study
pHGE-CydX-YFP_N	pHGE-P*tac* expressing CydX-YFP_N	This study
pHGE-TatA-YFP_N-TatA-YFP_C	pHGE-DP*tac* expressing TatA-YFP_N and TatA-YFP_C fusion proteins	This study
pHGE-CydA-YFP_N-CydB-YFP_C	pHGE-DP*tac* expressing CydA-YFP_N and CydB-YFP_C fusion proteins	This study
pHGE-CydX-YFP_N-CydA-YFP_C	pHGE-DP*tac* expressing CydX-YFP_N and CydA-YFP_C fusion proteins	This study
pHGE-CydX-YFP_N-CydB-YFP_C	pHGE-DP*tac* expressing CydX-YFP_N and CydB-YFP_C fusion proteins	This study

each sample was spotted onto LB plates w/o 5 mM nitrite. The plates were incubated for 24 h or longer before being read. For each strain, experiment was performed in triplicate and repeated independently at least three times.

2.4. Cytochrome oxidase activity assay

Quantitative analysis of quinol oxidase activity was assayed with solubilized membranes, which were prepared with a proper amount of cells grown under microaerobic conditions [17]. Cell pellets were resuspended in 20 mM Tris–HCl (pH 7.6) supplemented with DNase I and protease inhibitors and disrupted by French pressure. After removal of debris and unbroken cells, the membranes were pelleted by ultracentrifugation for 1 h at 230,000 ×*g* at 4 °C and subsequently resuspended in 20 mM Tris–HCl pH 7.6 with 5% glycerol to a protein concentration of 10 mg/ml. Solubilization was performed with *n*-dodecyl β-D-maltoside (DDM) to a final concentration of 1% (w/v) on a rotary tube mixer for 2 h at 4 °C. The DDM-solubilized membranes were obtained by collecting the supernatant after ultracentrifuging for 1 h at 230,000 ×*g* at 4 °C. Quinol oxidase activity was assayed as a measure of oxygen consumption rates using an OxyGraph oxygen electrode (Hansatech) according to the method described previously [29].

2.5. RT-PCR

RT-PCR was employed to determine the organization of the *cyd* operon. Whole RNA was extracted from mid-log phase cells (~0.3 of OD_{600}) using Trizol (Invitrogen) and RNeasy Mini kit (Qiagen) as described before [30]. For RT-PCR reaction, cDNAs were obtained using a PrimeScript™ RT-PCR kit (Takara) according to product instruction and then used as the template for PCR amplification.

2.6. Site-directed mutagenesis

Site-directed mutagenesis was performed to replace the 1–6 amino acid residues of CydX by the counterpart of $YneM_{EC}$, resulting in fusion protein of $YneM_{EC}$ (1–6 a.a.) and CydX (7–38 a.a.), according to the method used before [31]. pHG102-*cydX*, was used as the template with a QuikChange II XL site-directed mutagenesis kit (Stratagene). Mutated PCR products were generated, subsequently digested by *Dpn*I, and transformed into *E. coli* WM3064. After sequencing verification, the resulting plasmid was transferred into the *S. oneidensis* strains by conjugation.

2.7. Antibiotic susceptibility assay

Mid-log phase cultures were used to prepare a decimal dilution series. 3 μl of each dilution was dropped on the LB plates supplemented with antibiotics of various concentrations. The plates were incubated for 18 h at 30 °C and then photographed.

2.8. Expression of GFP fusions and quantification of fluorescence

GFP fusion proteins were prepared as described previously [32]. In brief, DNA fragments containing the gene of interest were PCR amplified with specifically designed primers, allowing the first-round products to be joined by a second round of PCR. The PCR fusions were cloned into pHG102 using standard methods, and transformed into *E. coli* WM3064 [32]. After verification by sequencing, the resultant vectors were moved into *S. oneidensis* strains by conjugation.

To observe the expression of cloned fusions, mid-log phase cultures (~0.3 of OD_{600}) in LB broth were collected. 100 μl of the culture was dropped onto a layer of 3% agar on a slide for immobilization. Once the droplet dried, a glass coverslip was placed on top. The expression and localization of GFP fusions were visualized using a Zeiss LSM-510 confocal laser scanning microscope equipped with a 63× oil immersion objective (numerical aperture: 1.4). GFP was excited using 488-nm irradiation from an argon ion laser and fluorescent emission was monitored by collection across windows of 505 to 530 nm. To quantify, mid-log phase cultures of each test strain carrying GFP fusions were collected, washed with phosphate-buffered saline containing 0.05% Tween 20, and resuspended in the wash buffer to an OD_{600} of 0.1. 100 μl cell suspensions were transferred into black 384-well plates at various time intervals, and fluorescence was measured using a fluorescence microplate reader (M200 Pro Tecan) with excitation at 485 nm and detection of emission at 515 nm. The relative signal intensities were calculated by normalizing test strains carrying various fusions to WT producing CydX-GFP.

2.9. BiFC analysis

Bi-molecule fluorescence complementation (BiFC) assays were designed and carried out according to the standard protocol [33]. For the assay, an isopropyl β-D-1-thiogalactopyranoside (IPTG) inducible expression system which contained two highly active promoters was developed in this study. Plasmid pHGE-P*tac*[32] was digested with *Bam*HI and *Hind*III and ligated to a DNA fragment containing P*tac* and a MCS generated by annealing oligonucleotides P*tac*-MCS-F/R, producing pHGE-DP*tac*. The plasmid, verified by sequencing, contains two P*tac* promoters in tandem, each followed by a MCS. The newly introduced MCS includes *Xba*I, *Age*I, *Xma*I, *Kpn*I and *Nde*I, embedded in the reverse primer. To prepare constructs for the BiFC assay, fragments for the gene of interest were PCR amplified and fused in the second round PCR, generating TatA-YFP_N, TatA-YFP_C, CydA-YFP_N, CydA-YFP_C, CydB-YFP_C, and CydX-YFP_N. Each PCR fusion was inserted after one of two P*tac* promoters within pHGE-DP*tac*, resulting in BiFC constructs TatA-YFP_N-TatA-YFP_C, and CydA-YFP_N-CydB-YFP_C, CydX-YFP_N-CydA-YFP_C, and CydX-YFP_N-CydB-YFP_C, and transformed into *E. coli* WM3064. After verification by sequencing, the resultant vectors were moved into *S. oneidensis* strains by conjugation. For the expression of cloned fusions, 0.1 mM IPTG was added to mid-log phase cultures (~0.3 of OD_{600}). The cultures were incubated at 200 rpm at 30 °C for 2 h. After induction, 100 μl of the culture was dropped onto a layer of 3% agar on a slide for immobilization. Once the droplet dried, a glass coverslip was placed on top. Expression and localization of YFP fusions were visualized using the Zeiss LSM-510 confocal laser scanning microscope as described above.

2.10. Protein analysis

SDS-polyacrylamide gel electrophoresis (SDS-PAGE) and Western blotting assay were performed as described previously [32]. Protein concentration was monitored by a GE NanoVue Spectrophotometer and/or using a Bradford assay with BSA as a standard (Bio-Rad). In brief, mid-log phase cultures (~0.3 of OD_{600}) were collected by centrifugation either directly or after 2 h induction by various concentrations of IPTG, and the resulting cell pellets were washed twice with phosphate-buffered saline (PBS) and then subjected to SDS-PAGE (12%). After membrane transfer for 2 h at 60 V using a Criterion blotter (Bio-Rad), the blotting membrane was probed with the primary antibody mouse anti-eGFP-tag monoclonal antibody (GenScript) and then the second antibody goat anti-mouse IgG-HRP (horse radish peroxidase) (Roche Diagnostics). Detection was performed using a chemiluminescence Western blotting kit (Roche Diagnostics) in accordance with the manufacturer's instructions and images were visualized with the UVP Imaging System. Gel band intensities were quantified with ImageJ software (http://imagej.nih.gov/ij).

2.11. Bioinformatics and statistical analyses

Transmembrane protein topology was predicted using Phobius [34] and presented using Protter [35]. Sequences of CydX proteins for

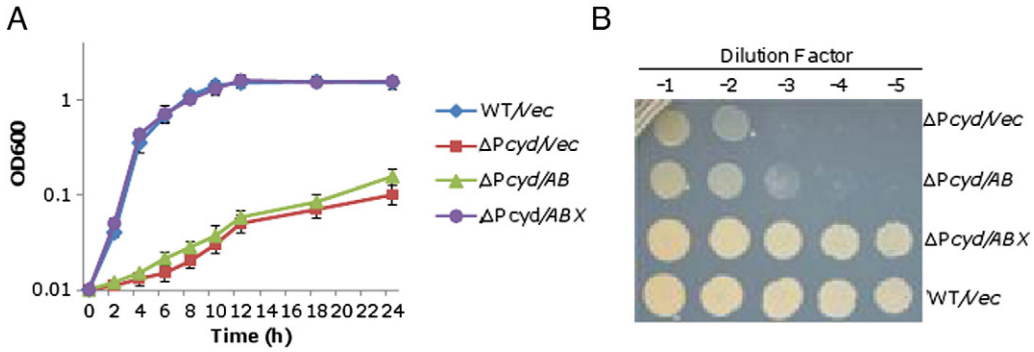

Fig. 1. Successful complementation of the P*cyd* mutant by the *cydAB-SO3284* genes but not the *cydAB* genes. (A) Growth of the *S. oneidensis* WT and ΔP*cyd* strains in the presence of nitrite. All strains were grown in LB broth supplemented with 5 mM nitrite under aerobic conditions and the optical density of cultures at 600 nm (OD_{600}) was recorded. (B) Nitrite susceptibility assay. Cultures of the mid-log phase were adjusted to similar optical densities and diluted in series, and 5 μl of each dilution was dropped onto LB plates containing 5 mM nitrite. The plates were incubated at 30 °C and photos were taken 24 h later. In both panels, AB, ABX, and Vec represent *cydAB*, *cydAB-SO3284*(*cydX*), and empty vector, respectively. All experiments were performed at least three times independently.

alignment were obtained from GenBank and alignment was performed using Clustal Omega (http://www.ebi.ac.uk/Tools/msa/clustalo). For statistical analysis, values are presented as means ± SD (standard deviation). Student's *t*-test was performed for pairwise comparisons of groups.

3. Results

3.1. Deletion of the SO3284 gene results in elevated susceptibility to nitrite

In our prior studies, we found that transcription of the *S. oneidensis cyd* operon (*cydAB*), relies on cyclic AMP receptor protein (Crp) [17,18,36]. During our investigation into the regulatory mechanism, we constructed mutant strains lacking the promoter of the *cyd* operon (ΔP*cyd*), which were highly sensitive to nitrite as expected. To confirm that the observed phenotype was due to the mutation *per se*, the ΔP*cyd* strain was subjected to genetic complementation. As reported previously [17,18], the *bd* oxidase confers *S. oneidensis* resistance to nitrite (Fig. 1). Interestingly, the *cydAB* genes under the control of constitutively active promoter, *S. oneidensis arcA*[28], within vector pHG102 failed to correct the mutant phenotype. In an attempt to explain this result, we noticed that the *ybgT* gene of *E. coli*, an ORF immediately downstream of the *cydAB* genes, encodes a membrane-anchored protein of 37 residues although its function was unknown then [22]. In the same locus of the *S. oneidensis* genome, there seems an ORF, namely *SO3284*, encoding a protein of 38 residues sharing a high level of sequence similarity to *E. coli* YbgT (refer to Fig. 3A). As this ORF is only 18 bp downstream of the stop codon of the *cydB* gene, we reasoned that SO3284 may be functionally associated with the cytochrome *bd* oxidase. To test this hypothesis, we cloned *cydAB-SO3284* into pHG102 as described above and tested its ability to restore the resistance of the ΔP*cyd* strain to nitrite (Fig. 1). This time, the phenotype resulting from the P*cyd* deletion was fully corrected by the expression of the cloned genes, indicating that SO3284 is crucial for the function of the cytochrome *bd* oxidase in *S. oneidensis*.

To confirm the functional involvement of SO3284 in the cytochrome *bd* oxidase, we created in-frame deletion strains lacking *SO3284* and a fragment covering the *cydAB-SO3284* genes, namely Δ*SO3284* and Δ*cyd*, respectively. In the presence of 5 mM nitrite, we observed that the growth of both mutants was severely defective (Fig. 2A). These expected phenotypes of growing defect were fully complemented when the corresponding gene(s) was expressed *in trans* within pHG102. However, levels of growth defects resulting from the deletion of the *cydAB-SO3284* genes and the *SO3284* gene alone were not identical. This was more evident on plates for assessing nitrite susceptibility (Fig. 2B). Loss of all three genes led to a hypersensitivity to nitrite that was more severe than that observed for the Δ*SO3284* strain. To provide direct evidence for the role of SO3284 in the activity of the *bd* oxidase, quinol oxidase activity of the membranes from microaerobic cultures was determined by measuring O_2 uptake with ubiquinol-1 as the electron donor (Table 2). The Δ*cyd* strain hardly retained any ubiquinol-1 oxidase activity, about 1% relative to that of WT; the same result was obtained from the removal of CydA and CydB subunits. In the case of the Δ*SO3284* strain, the residual activity was observed, approximately 10% relative to WT. All together, these data indicate that the cytochrome *bd* oxidase retains some residual activity in the absence of SO3284.

To further confirm this, we intended to cross-complement the Δ*SO3284* strain with its *E. coli* counterparts. The *E. coli* genome encodes two cytochrome *bd* oxidase complexes, CydAB-YbgT-YbgE and AppCB-YccB-AppA. YbgT and YccB share 61% and 40% sequence identity to SO3284, respectively. Both YbgT and YccB have been recently demonstrated to be essential for CydAB and AppCB complexes respectively,

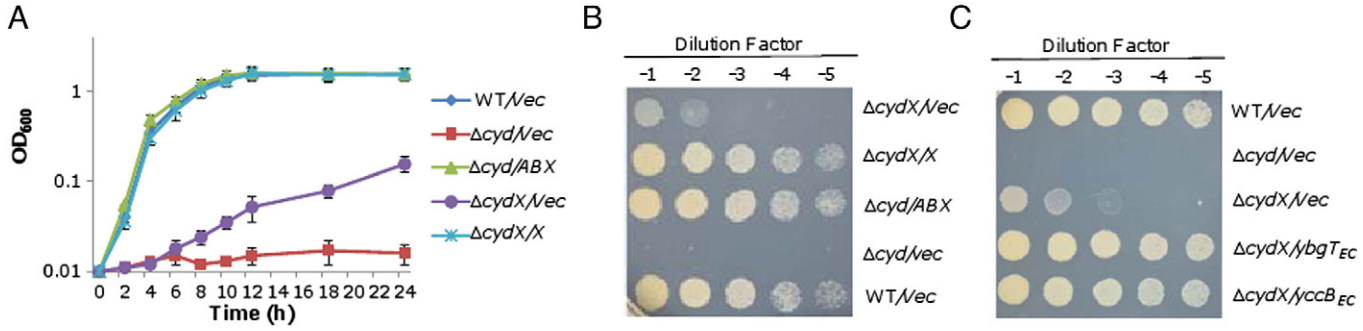

Fig. 2. Phenotypes of various *cyd* mutants. (A) Growth of the *S. oneidensis* WT and Δ*cyd* strains in the presence of nitrite. All strains were grown in LB broth supplemented with 5 mM nitrite under aerobic conditions and the optical density of cultures at 600 nm (OD_{600}) was recorded. (B and C) Nitrite susceptibility assay. Experiments were performed the same as described in Fig. 1B. In both panels, ABX, and Vec represent *cydAB-SO3284*(*cydX*), and empty vector, respectively. All experiments were performed at least three times independently.

Table 2
Quinol oxidase activities in membrane preparations of *S. oneidensis* strains.[a]

Strain	Ubiquinol-1 oxidase activity (nmol $O_2 \cdot min^{-1} \cdot mg\ protein^{-1}$)	
	Empty vector	Complementation by *cydAB*
WT	288 ± 22	–
Δ*cyd*	3 ± 0.5	6 ± 1
Δ*cydAB*	6 ± 1	314 ± 28
Δ*SO3284*	26 ± 3	31 ± 5

[a] Cells grown under microaerobic conditions; data presented as means ± SD of at least three independent experiments.

and more importantly YccB is able to complement an *ybgT* mutant [25]. We therefore cloned these two genes into pHG102, and the resulting plasmids were introduced into the Δ*SO3284* strain for the nitrite sensitivity assay. As shown in Fig. 2C, both genes conferred the Δ*SO3284* strain nitrite resistance of the WT level. In addition, the expression of either gene in the Δ*SO3284* strain resulted in growth in the presence of 5 mM nitrite comparable to that of WT (data not shown). These data collectively indicate that SO3284 is an essential functional part of cytochrome *bd* oxidase in *S. oneidensis*. During this study, a YbgT homologue in *B. abortus* was renamed as CydX and so was *E. coli* YbgT [27,28], to be consistent, the same nomenclature was used here for SO3284.

3.2. The cydX gene is co-transcribed with the cydAB genes

Next, we set out to determine whether the *cydX* gene is co-transcribed with the *cydAB* genes. In the *S. oneidensis* genome, the *cydX* gene is at the immediate downstream of the *cydAB* genes, followed tightly by a putative transcriptional terminator, the same way homologues in *E. coli* are organized (Fig. 3A). Whole RNA was extracted from both *S. oneidensis* and *E. coli* and RT-PCR was performed. For *S. oneidensis*, we were able to obtain clear bands of correct size with the forward primer within the *cydB* gene and the reverse primer within either the *cydB* or *cydX* gene, suggesting that the *cydABX* genes belong to a single operon (Fig. 3B). No band was obtained when the reverse primer was located after the transcriptional terminator, confirming the existence of a functional terminator immediately after the operon. The same results were obtained in *E. coli* (Fig. 3B), suggesting that the genes for the cytochrome *bd* oxidases are similarly organized. Given that no band was detected in an RNase-treated control reaction, it is unlikely that the signal is due to genomic DNA contamination (data not shown). It is worth mentioning that another small ORF *ybgE* following the *cydX* (*ybgT*) gene is previously reported being co-transcribed within the same *cyd* operon in *E. coli*[20]. However, our results suggest that the gene is independently transcribed because we did obtain a band with the primer within the *ybgE* gene (Fig. 3B). While this discrepancy may simply be resulted from different methods used, it is clear that YbgE has no role in the function of the *bd* oxidase [25].

3.3. CydX is required for the in vivo function of the CydAB complex

The enhanced activity of the CydAB complex in the presence of CydX can be explained by two distinct mechanisms: a required component of the CydABX complex and a factor that simply stimulates the oxidase activity but is not critical for its function. To determine through which mechanism CydX plays its role, we tested the ability of CydAB overproduction to suppress the nitrite sensitive phenotypes associated with a *cyd* defect using two different vectors. The gene of interest under the

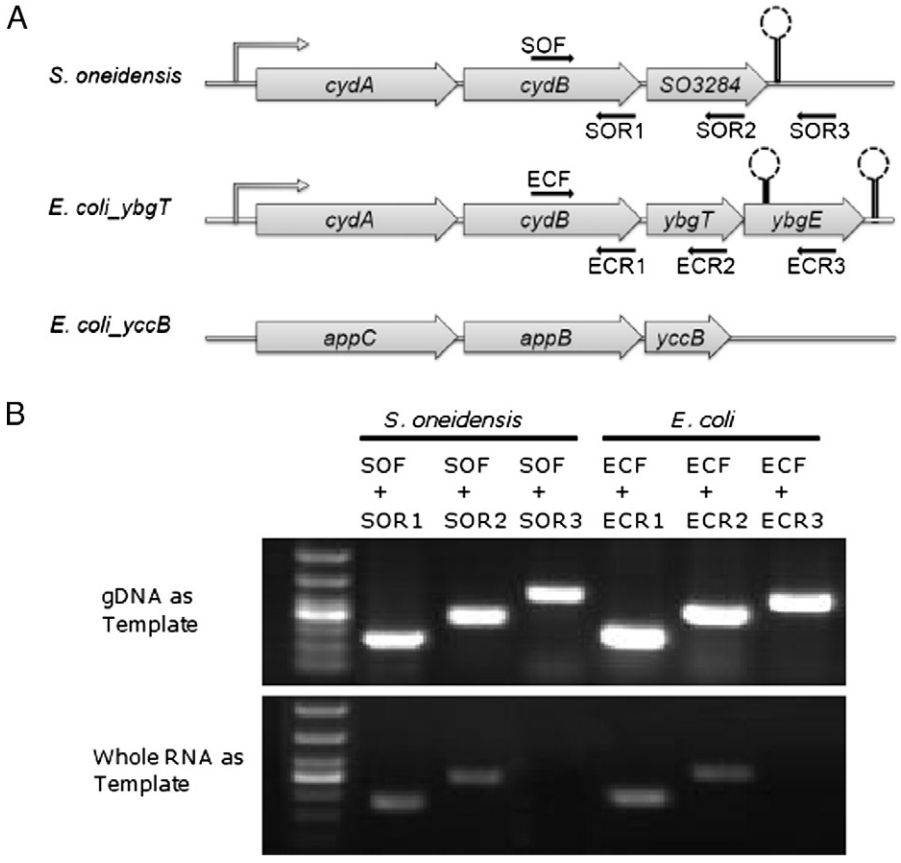

Fig. 3. The *cydX* gene is co-transcribed with the *cydAB* genes. (A) Organization of the cytochrome *bd* oxidase operons in *S. oneidensis* and *E. coli*. Genes are not drawn to scale as *cydX*, *ybgT*, and *yccB* are too short to be labeled clearly. The transcription terminator is marked with a stem-ring structure. The location of primers used is given. (B) RT-PCR results. Total RNAs were extracted from the mid-log phase cultures. RT-PCR experiments were carried out as described in Materials and methods. All experiments were performed at least three times independently and similar results were obtained. These images were cropped.

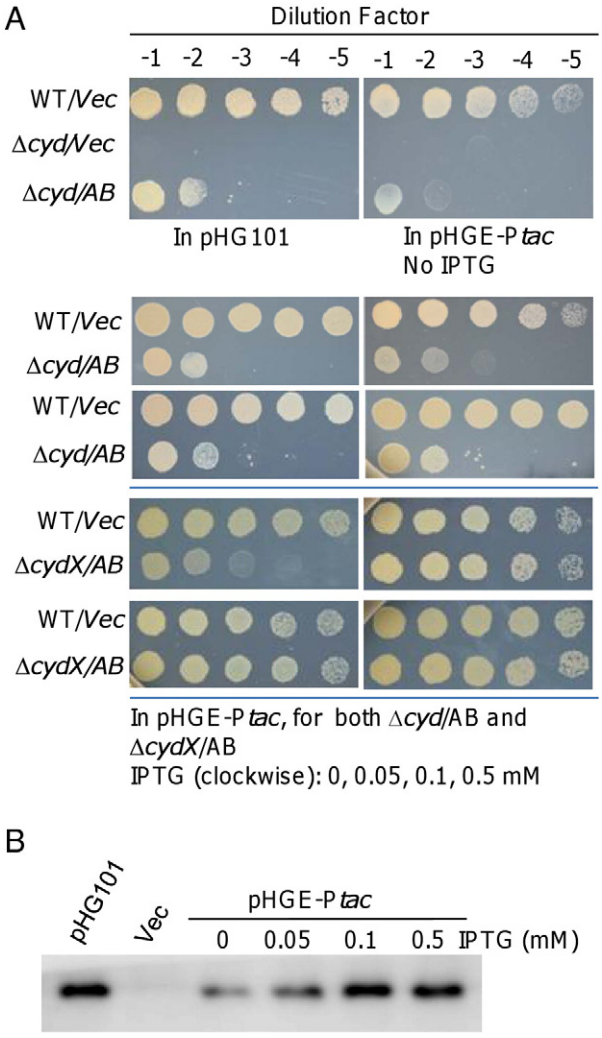

Fig. 4. CydX is crucial for function of the cytochrome *bd* complex. (A) Nitrite susceptibility assay. Experiments were performed the same as described in Fig. 1B. (B) To determine the extent of CydAB overproduction in the cultures from (A), extracts were prepared from cells harvested at the mid-log phase. Immunoblot analysis of extracts containing the same amount of proteins was then performed to determine the levels of fused GFP. In both panels, AB and Vec represent *cydAB* and empty vector, respectively. All experiments were performed at least three times independently and similar results were obtained. These images were cropped.

control of its native promoter in multiple-copy vector pHG101 has been repeatedly shown to have overproduction by approximately 5 to 15-fold [27,31,36]. Apparently, the overproduction of CydAB from pHG101, was not sufficient to suppress the nitrite hypersensitive phenotype of the Δ*cyd* cells (Fig. 4A). We then utilized an IPTG-inducible expression vector in which the gene of interest is under the control of the P*tac* promoter [32]. Although levels of CydAB produced by IPTG induction varied more than 10-fold (quantified by using ImageJ), no enhancement in nitrite resistance was observed (Fig. 4A and B). When the same vector was introduced to the Δ*cydAB* strain, IPTG at 0.05 mM was sufficient to induce nitrite resistance of the WT level. Notably, a modest increase in nitrite resistance was observed without IPTG, a phenomenon due to the leakiness of the P*tac* promoter as reported previously [32,37]. Importantly, Western blotting analysis of GFP fused to CydAB revealed increased production of expected levels (Fig. 4B). Based on these data, we conclude that CydX is essential for the *in vivo* function of their cognate CydA and CydB subunits as opposed to factors that simply stimulate oxidase activity but are not critical for their function.

3.4. Membrane localization of CydX is independent of the CydAB complex

CydX is predicted to be a membrane protein with its N-terminal as the single transmembrane domain and its C-terminal exposed in the cytosol (C_{in}–N_{out} orientation). This feature is experimentally demonstrated in *E. coli* CydX using CydX-GFP fusion proteins because GFP is only fluorescent in the cytoplasm [22]. As the orientation of CydX is particularly important for the determination of its membrane localization, we utilized β-lactamase fusions for verification. In *S. oneidensis*, the periplasmically located β-lactamase, encoded by the *blaA* gene, is the primary enzyme for degradation of β-lactam antibiotics [38]. BlaA was fused to either end of CydX and the resulting proteins were expressed in a BlaA-deficient strain (Δ*blaA*). While all test strains displayed identical growth on ampicillin-free plates production of fused proteins rendered Δ*blaA* cells substantially different susceptibilities to the antibiotics. In the presence of 25 μg/ml ampicillin, cells producing CydX-BlaA remained sensitive to ampicillin, a phenomenon observed from those carrying empty vector (Fig. 5A). In contrast, when BlaA-CydX was produced, the Δ*blaA* strain exhibited strong resistance to ampicillin, exceeding that of WT significantly, apparently from overproduction of BlaA. These data conclude that CydX is orientated in the C_{in}–N_{out} manner.

As CydX is vital to the function of the cytochrome *bd* oxidase, we intended to know whether its localization is dependent on components CydA and/or CydB. To this end, we used GFP fusions. As shown in Fig. 5B, the CydX-GFP fusion proteins were located in the membrane in the WT, Δ*cydA*, Δ*cydB*, and Δ*cyd* strains whereas GFP-only proteins filled up the cytoplasm. Consistent with its C_{in}–N_{out} orientation, cells producing GFP-CydX fusion proteins were extremely low in fluorescence. By quantification, levels of CydX-GFP fusions were similar in all of these strains, but the signal intensity of GFP-only was significantly stronger, over 5-fold than those of CydX-GFP fusions. This observation gained support from Western blotting against GFP (Fig. 5C). Levels of both CydX-GFP and GFP-CydX fusion proteins were comparable within all test strains. Consistently, the amount of GFP-only proteins was higher than GFP fusions. These data indicate that the CydAB complex has little influence on the stability of CydX (Fig. 5B). Altogether, these data suggest that CydX may not need other components of the cytochrome *bd* oxidase for its production, membrane targeting, and integration.

3.5. Complexation of CydA and CydB is independent of CydX

Several small proteins found in membrane complexes have been shown to act as stabilizing factors [39]. For instance, PetG and PetN in the cytochrome *b6f* complex were reported to be involved in assembly and stability of the complex. Inspired by this, we attempted to find out whether or not CydX acts as a stabilizing factor to help assemble the oxidase complex using the BiFC technology. The BiFC technology, a key technique to visualize interactions between membrane-bound proteins, is based on reconstitution of an intact fluorescent protein when two complementary non-fluorescent fragments are brought together by a pair of interacting proteins [33]. To do this, we first developed a plasmid pHGE-DP*tac*, which contains two P*tac* promoters in tandem such that two protein fusions for BiFC can be produced at similar levels. To validate the system, TatA, a major component of the TAT (Twin-Arginine Translocation) system, was fused to the N- or C-terminal part of YFP, resulting in constructs TatA-YFP_N, TatA-YFP_C, and TatA-YFP_N-TatA-YFP_C within pHGE-DP*tac* independently. *E. coli* TatA, identical to *S. oneidensis* TatA in structure and function, can form homopolymeric pores as protein translocation passages in the cytoplasmic membrane [32,40]. Constructs containing the N- or C-terminal part of YFP alone, TatA-YFP_N and TatA-YFP_C, did not show any fluorescence (Fig. 6A). On the contrary, fluorescence was observed from construct TatA-YFP_N-TatA-YFP_C when IPTG was added in the medium, indicating efficacy of this technique in *S. oneidensis*.

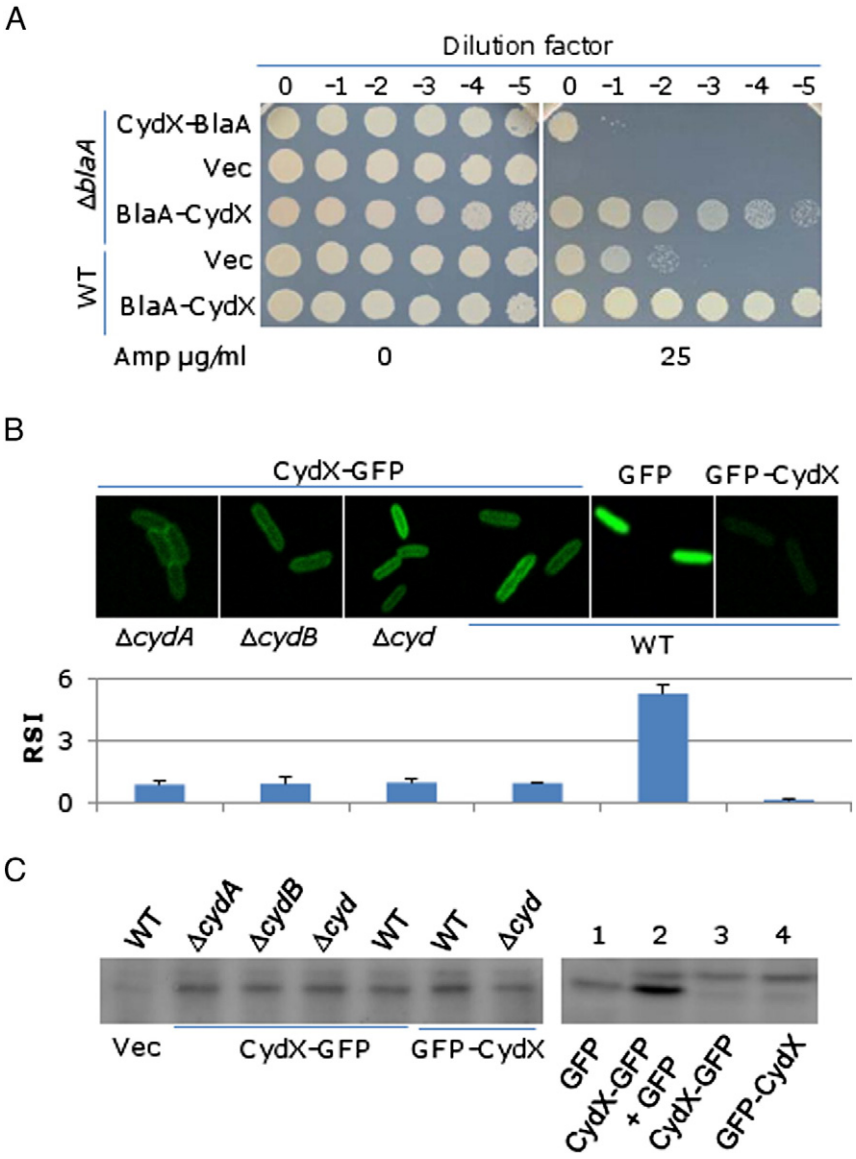

Fig. 5. Production and membrane integration of CydX are independent of the CydAB subunits. (A) Location of β-lactamase fusions. Both WT and Δ*blaA* strains expressing indicated fusions or not were used in the assay. 3 μl of mid-log phase culture of decimal dilution series was dropped on the LB plates supplemented with ampicillin or not. The plates were incubated for 18 h at 30 °C. (B) Location of GFP fusions. Fluorescence images of the WT, Δ*cydA*, Δ*cydB*, and Δ*cyd* strains expressing indicated fusions were shown. Cells at the mid-log phase were visualized under a Zeiss LSM-510 confocal laser scanning microscope. Signal intensities of samples were quantified using a fluorescence microplate reader. The relative signal intensity (RSI) was calculated by normalizing the signal intensity of each sample to that of WT expressing CydX-GFP and presented underneath the corresponding sample. Error bars represent the standard deviation from at least three independent experiments. (C) To determine levels of GFP fusion production in the cultures from (B), extracts were prepared from cells harvested at the mid-log phase. Immunoblot analysis of extracts containing the same amount of proteins was then performed to determine the levels of fused GFP. To show relative amounts of fusion proteins, indicated fusions from WT were artificially mixed and loaded in numbered lanes on the right. 1. 5-fold dilution of GFP-only extract, 2. mixture of same volume of GFP-only and CydX-GFP extracts, 3. CydX-GFP extract, and 4. GFP-CydX extract. In all panels, Vec represents empty vector. Similar results were obtained for at least three independent experiments. These images were cropped.

Given that C-termini of both CydA and CydB are exposed in the cytoplasm [1], the N- and C-terminal parts of YFP were engineered to the C-end of CydA and CydB, respectively, resulting in CydA-YFP_N, CydB-YFP_C, and CydA-YFP_N-CydB-YFP_C. These constructs were then introduced into both WT and Δ*cydX* strains. As expected, no fluorescence was observed from CydA-YFP_N and CydB-YFP_C (Fig. 6B). In the case of CydA-YFP_N-CydB-YFP_C, fluorescence of similar levels was observed from WT, Δ*cydX*, and Δ*cyd* strains, indicating that the formation of the CydAB complex is independent of CydX. In *E. coli*, CydX has been suggested to be co-existing with both CydA and CydB by an *in vitro* pull-down analysis [25]. However, *in vivo* evidence is lacking. We therefore made an attempt to address this with BiFC technology. A structure for expressing CydX-YFP_N was constructed. When paired with CydA-YFP_C or CydB-YFP_C, CydX-YFP_N was able to generate detectable fluorescence (Fig. 6B), supporting the notion that the small subunit coexists with the CydAB complex. These results, altogether, exclude the possibility that CydX functions as a stabilizing factor in the assembly of the CydAB complex.

3.6. The conserved N-terminal transmembrane region of CydX is important to function

CydX is conserved across Proteobacteria, with length varying between 30 and 50 amino acid residues. While *Shewanella* CydX proteins are nearly identical, a cross-species comparison shows that the N-terminal segment (1–25 residues) is highly conserved whereas the remaining C-terminal sequence less (Fig. 7A and Fig. S1). The importance of conserved residues within *E. coli* CydX has been recently

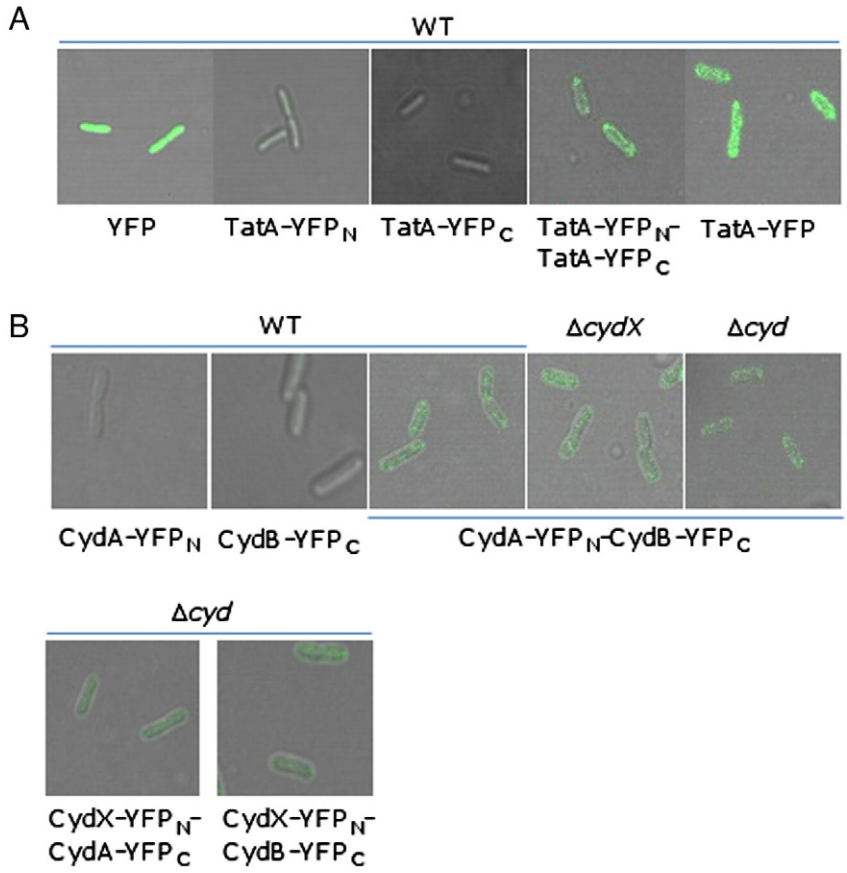

Fig. 6. Complexation of CydAB is independent of CydX. (A) Validation of constructs for BiFC assay. Cells expressing indicated fusions were prepared as described in Fig. 5 and visualized under a Zeiss LSM-510 confocal laser scanning microscope. (B) Complexation of CydAB. Strains of various genetic backgrounds expressing indicated fusions were assayed as in (A). All experiments were performed at least three times independently and similar results were obtained.

examined [25]. Surprisingly, many of the highly conserved residues are not critical to functionality, suggesting a high degree of sequence flexibility. Given that the well-conserved N-terminal region of CydX proteins is predicted to be a single transmembrane domain (Fig. 7B), we reasoned that this segment should be particularly important for function. To test this, we constructed two hybrid proteins, YneM$_N$-CydX$_C$ (YC) and CydX$_N$-AcrZ$_C$ (CA), the former retaining the original CydX C-terminal sequence but acquiring the transmembrane N-terminal segment from small protein YneM of *E. coli* and the latter having the CydX N-terminal segment and the C-terminal segment of small protein *E. coli* AcrZ fused. While YneM is functionally unknown at present, AcrZ is an accessory protein of AcrAB-TolC efflux pump, facilitating the pump in the recognition and export of a subgroup of substrates [41]. The common feature among these three small proteins is that they are all membrane-associated proteins with the same orientation [22]. When YneM$_N$-CydX$_C$ was expressed, cells lacking CydX was as sensitive to nitrite as those carrying the empty vector (Fig. 7C). On the contrary, the presence of CydX$_N$-AcrZ$_C$ enabled the Δ*cydX* strain to resist nitrite at levels similar to those of WT. To further assess effects of these hybrid proteins, we compared the growth of the Δ*cydX* strain carrying one of these three proteins. As expected, the Δ*cydX* strain carrying CydX$_N$-AcrZ$_C$ was able to flourish in the presence of 5 mM nitrite despite a slightly decreased growth rate whereas YneM$_N$-CydX$_C$ cells lacking CydX were incapable of growing (Fig. 7D). These data support that the N-terminal transmembrane segment is crucial for functionality in contrast to the much less significance of the cytosol segment.

The N-terminal segment can be further divided into a periplasmic pentapeptide and a transmembrane peptide. Interestingly, the periplasmic pentapeptide (MWYFT) is rich in aromatic residues (Fig. 7A). In addition, the sixth residue (W) is also an aromatic residue and these aromatic residues are among the most conserved. We therefore were interested in finding out the importance of the periplasmic pentapeptide to CydX function. To minimize conformational alternation, residues WYFTW of CydX were replaced by residues LGNMN of *E. coli* YneM because these two pentapeptide segments are similarly exposed into the periplasm, at least in the context of the structural prediction (Fig. 7B). When the resulting mutant protein YneM$_P$-CydX$_R$ (Peri) was expressed from pHG102, the Δ*cydX* strain displayed elevated resistance to nitrite, albeit still lower than cells carrying the WT CydX (Fig. 6C). Consistent with this observation, the YneM$_P$-CydX$_R$ proteins partially restored growth of the Δ*cydX* strain in the presence of 5 mM nitrite. Altogether, these data suggest that both periplasmic and transmembrane segments are important for the functionality of CydX in *S. oneidensis*.

4. Discussion

Historically functions of small proteins have been understudied for several reasons. Approaches adopted in protein biology tend to be optimized for studying large molecules and small proteins are often missed or ignored in proteomic studies [42]. Genome annotation algorithms may not be sensitive enough for small ORFs as they lack sufficient sequences for domain and homology determination [43,44]. In addition, it is difficult to catch small genes using random genetic screens because of their short coding sequences [45]. Moreover, disruption of many predicted small ORFs may not cause apparent phenotypes under routine experimental conditions and to screen for specific stimuli required for a distinct phenotype remains a challenging task to date [41,45–47]. This scenario is further compounded by gene duplication

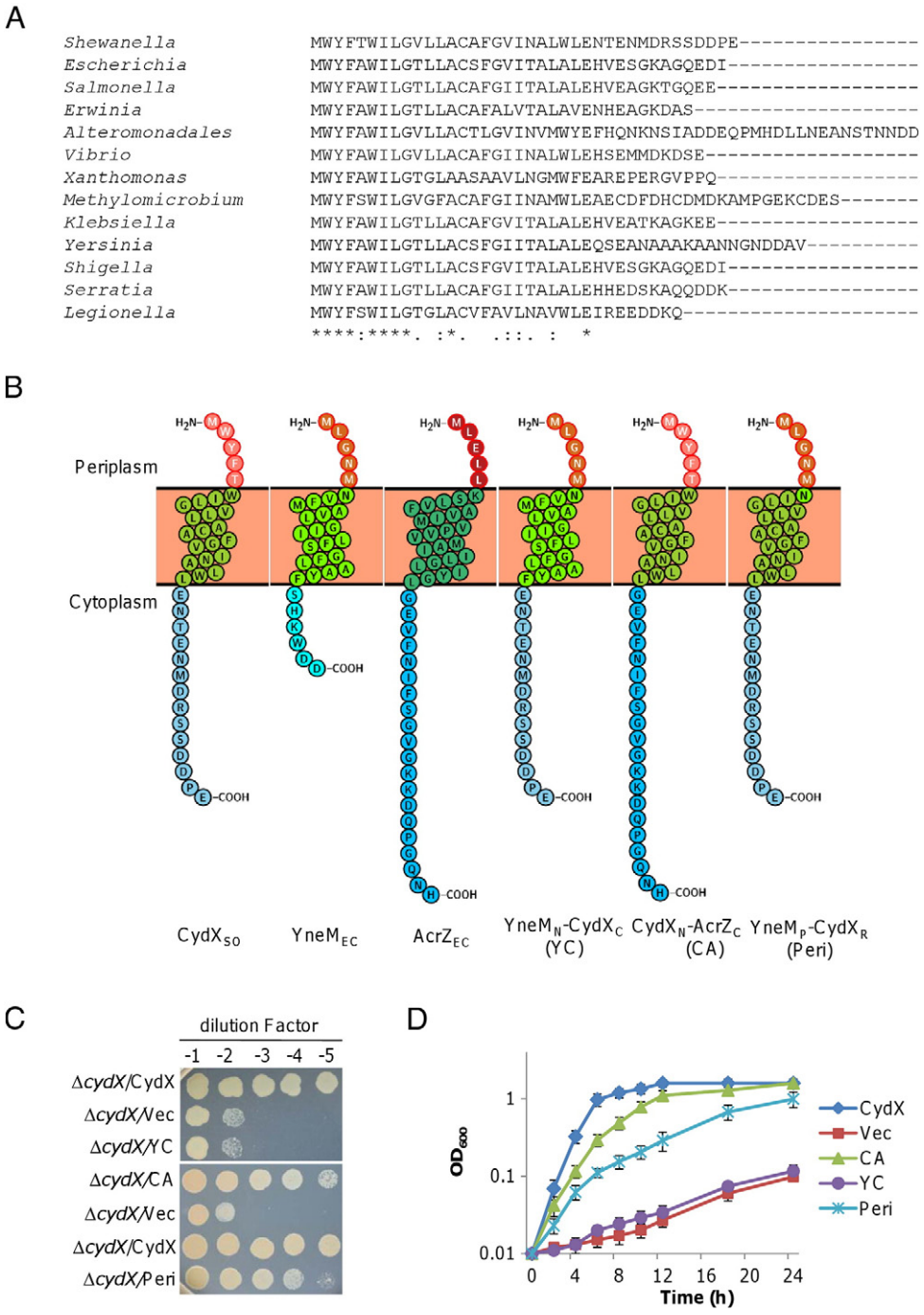

Fig. 7. Functional analysis of CydX by segment replacement. (A) Alignment of the sequences of select CydX homologues. Homologues were obtained using a Blastp search against database in NCBI GenBank using the *S. oneidensis* CydX sequence. (B) Predicted sequence features of small proteins used in the segment replacement experiment. Sequence features were predicted using Phobius and presented using Protter. Fusion proteins YneM$_N$-CydX$_C$ (YC), CydX$_N$-AcrZ$_C$ (CA), and YneM$_P$-CydX$_R$ (Peri) were also shown. (C) Nitrite susceptibility assay. Experiments were performed the same as described in Fig. 1B. (D) Growth of the *S. oneidensis* strains in the presence of nitrite. All strains were grown in LB broth supplemented with 5 mM nitrite under aerobic conditions and the optical density of cultures at 600 nm (OD$_{600}$) was recorded. In B, C, and D, Vec, YC, CA, and Peri represent empty vector, YneM$_N$-CydX$_C$, CydX$_N$-AcrZ$_C$, and YneM$_P$-CydX$_R$, respectively. All experiments were performed at least three times independently.

and function redundancy, a widespread phenomenon that has limited the effectiveness of genetic analysis. As a result, loss of either one can be functionally complemented by the other. A good and ready example is two functionally overlapping cytochrome *bd* oxidases in *E. coli*. The small ORF *cydX* has been identified for 17 years [20], but its function stays unclear for a similarly long time. Given its genetically close association with the cytochrome *bd* oxidase, prediction has been made that CydX could be a part of the enzyme complex but direct evidence emerged just recently [24,25].

Cytochrome *bd* respiratory terminal oxidases are a large family of oxygen reductase different from HCO and alternative oxidase (AOX) families [1]. It has been proposed that the quinol:oxygen reductase works by transferring four electrons from either ubiquinol or menaquinol, or in the case of cyanobacteria, plastoquinol, sequentially through its two active reaction centers comprised of all its prosthetic hemes, and finally to molecular oxygen. The first reactive center is heme b_{558}, which resides in the large subunit CydA, while the other center is at the interface of CydA and CydB, containing heme b_{595} and heme

d[1]. The oxidase complex is able to establish a transmembrane proton gradient by charge separation, that is, releasing protons from quinol into the periplasm and consuming protons in the cytoplasm to form water when reducing oxygen [48].

Although substantially impaired in function, the *S. oneidensis* cytochrome *bd* oxidase without CydX is still able to confer significantly elevated resistance to nitrite compared to the loss of the entire cytochrome *bd* oxidase, indicating that a functional complex can be assembled by the large subunits CydA and CydB only. Consistently, membrane targeting and integration of CydX with respect to large subunits appear to be reciprocally independent of each other as revealed by GFP fusions and BiFC analysis. In the complex, CydX is proposed to be located in the interface between CydA and CydB as CydX interacts with both large subunits directly [25]. We envision that this arrangement would allow CydX to be part of the proposed proton passage, through which protons in the cytoplasm can be streamed to the oxygen reducing site, the bi-heme b_{595}–*d* reactive center [19,49,50]. This hypothesis is supported by the appearance of multiple acidic residues (6 out of 14) in the C-terminal which may help attract protons from the cytosol and the significant defect resulting from the C-terminal segment swapping between CydX and $AcrZ_{EC}$, which has 2 such residues in total of 20.

Meanwhile, a direct involvement of CydX in participating biochemical reaction cannot be superficially rejected. The 12th residue leucine was decisive for the activity of the complex although single-residue substitution of most conserved residues by alanine did not result in notable function loss [25]. In addition, the replacement of the 4th (Phe), 7th (Ile), and 21st (Ala by Gly) residues caused significant reduction in the enzymatic activity. These four residues may work in a coordinate manner as they are predicted to be located on the same side of the hydrophobic α-helix. The role of CydX as a critical subunit rather than a factor that simply stimulates the activity of the CydAB complex is further supported by the finding that the enzymatic activity of the CydAB complex did not significantly increase by overproduction. Similarly, the overproduction of CydX had little influence on the activity of the CydAB complex, at least in the context of growth and nitrite resistance.

A more attractive possibility is that CydX is critical to positioning and stabilization of the prosthetic hemes, especially heme *d*. As mentioned above, the oxidase contains three hemes, b_{558}, b_{595}, and *d*, and the latter two are believed to form a di-heme site for the reduction of oxygen [48,51]. Given that the location of all three hemes is predicted to be near the periplasmic surface [52], it is conceivable that the transmembrane segment as well as residues in the periplasm is particularly critical. Indeed, our results demonstrated that a combination of the transmembrane helix and the N-terminal periplasmic overhang is essential for the enzymatic activity and the periplasmic part alone is more crucial than the much longer C-terminal segment with respect to functionality. It is worth mentioning that this periplasmic peptide is dominated by aromatic residues, whose large side chain may have a role in structural orientation. Finally, CydX may function as a quinol (Q) stabilizer when it is being oxidized during charge separation, given the unusual co-occurrence of CydX and the long Q-loop in CydA, which connects transmembrane helices 6 and 7, and is directly involved in QH_2 binding and oxidation [53]. Based on the length of the Q-loop, bacteria hosting cytochrome *bd* oxidases can be divided into long and short Q-loop groups and the subgroup of CydA with long Q-loop is also mostly restricted in Proteobacteria, mainly γ and β groups [1,54]. Coincidently, CydX is seemingly restricted in Proteobacteria, largely γ-proteobacteria [25]. Therefore, it is reasonable to propose that extra effort from CydX is needed to stabilize quinol in the enlarged binding site (Q-loop) and that an enlarged binding site may be helpful to release oxidized quinone and thus increase the overall turnover of Q-pool. It should be noted that, while this manuscript was under preparation, another study on *E. coli* CydX was published [55]. Authors proposed that CydX is required for the stability of the di-heme active site, supporting our predicted mechanism that CydX is critical to positioning and stabilization of the prosthetic hemes.

Regardless of their precise biochemical function, the discovery of functionally critical accessory factors suggests new avenues for investigating the mechanisms by which small proteins influence the activity of large enzymatic complexes. This may be particularly valuable for the cytochrome *bd* oxidase because our current understanding of the enzyme is nearly entirely built on *in vitro* biochemical studies of the CydAB complex. Conceivably, the addition of CydX into the same experimental settings may alter some results and/or their explanations. Therefore, further biochemical research of the CydABX complex is much needed for clarification.

Acknowledgements

This research was supported by the National Natural Science Foundation of China (31270097), Major State Basic Research Development Program (973 Program: 2010CB833803), and Doctoral Fund of Ministry of Education of the People's Republic of China(20130101110142).

References

[1] V.B. Borisov, R.B. Gennis, J. Hemp, M.I. Verkhovsky, The cytochrome *bd* respiratory oxygen reductases, Biochim. Biophys. Acta 1807 (2011) 1398–1413.
[2] I. Belevich, V.B. Borisov, A.A. Konstantinov, M.I. Verkhovsky, Oxygenated complex of cytochrome *bd* from *Escherichia coli*: stability and photolability, FEBS Lett. 579 (2005) 4567–4570.
[3] I. Belevich, V.B. Borisov, D.A. Bloch, A.A. Konstantinov, M.I. Verkhovsky, Cytochrome *bd* from *Azotobacter vinelandii*: evidence for high-affinity oxygen binding, Biochemistry 46 (2007) 11177–11184.
[4] P.A. Cotter, S.B. Melville, J.A. Albrecht, R.P. Gunsalus, Aerobic regulation of cytochrome *d* oxidase (*cydAB*) operon expression in *Escherichia coli*: roles of Fnr and ArcA in repression and activation, Mol. Microbiol. 25 (1997) 605–615.
[5] V.B. Borisov, E. Forte, A.A. Konstantinov, R.K. Poole, P. Sarti, A. Giuffrè, Interaction of the bacterial terminal oxidase cytochrome *bd* with nitric oxide, FEBS Lett. 576 (2004) 201–204.
[6] V.B. Borisov, E. Forte, P. Sarti, M. Brunori, A.A. Konstantinov, A. Giuffrè, Redox control of fast ligand dissociation from *Escherichia coli* cytochrome *bd*, Biochim. Biophys. Res. Comm. 355 (2007) 97–102.
[7] V.B. Borisov, E. Forte, A. Davletshin, D. Mastronicola, P. Sarti, A. Giuffrè, Cytochrome *bd* oxidase from *Escherichia coli* displays high catalase activity: an additional defense against oxidative stress, FEBS Lett. 587 (2013) 2214–2218.
[8] E. Forte, V.B. Borisov, A. Davletshin, D. Mastronicola, P. Sarti, A. Giuffrè, Cytochrome *bd* oxidase and hydrogen peroxide resistance in *Mycobacterium tuberculosis*, mBio 4 (2013) e01006–e01013.
[9] Berney, M., Hartman, T.E., Jacobs, W.R. A *Mycobacterium tuberculosis* cytochrome *bd* oxidase mutant is hypersensitive to bedaquiline. *mBio* 5 (2014) e01275-14.
[10] A. Giuffrè, V.B. Borisov, M. Arese, P. Sarti, E. Forte, Cytochrome *bd* oxidase and bacterial tolerance to oxidative and nitrosative stress, Biochim. Biophys. Acta 1837 (2014) 1178–1187.
[11] S. Endley, D. McMurray, T.A. Ficht, Interruption of the *cydB* locus in *Brucella abortus* attenuates intracellular survival and virulence in the mouse model of infection, J. Bacteriol. 183 (2001) 2454–2462.
[12] M.G. Mason, et al., Cytochrome *bd* confers nitric oxide resistance to *Escherichia coli*, Nat. Chem. Biol. 5 (2009) 94–96.
[13] J.K. Fredrickson, et al., Towards environmental systems biology of *Shewanella*, Nat. Rev. Micro. 6 (2008) 592–603.
[14] J.F. Heidelberg, et al., Genome sequence of the dissimilatory metal ion-reducing bacterium *Shewanella oneidensis*, Nat. Biotech. 20 (2002) 1118–1123.
[15] H. Gao, et al., Impacts of *Shewanella oneidensis* *c*-type cytochromes on aerobic and anaerobic respiration, Microb. Biotech. 3 (2010) 455–466.
[16] G. Zhou, J. Yin, H. Chen, Y. Hua, L. Sun, H. Gao, Combined effect of loss of the caa_3 oxidase and Crp regulation drives *Shewanella* to thrive in redox-stratified environments, ISME J. 7 (2013) 1752–1763.
[17] H. Fu, et al., Crp-dependent cytochrome *bd* oxidase confers nitrite resistance to *Shewanella oneidensis*, Environ. Microbiol. 15 (2013) 2198–2212.
[18] H. Zhang, et al., Impacts of nitrate and nitrite on physiology of *Shewanella oneidensis*, PLoS ONE 8 (2013) e62629.
[19] V.B. Borisov, et al., Aerobic respiratory chain of *Escherichia coli* is not allowed to work in fully uncoupled mode, Proc. Natl. Acad. Sci. USA 108 (2011) 17320–17324.
[20] M.M. Muller, R.E. Webster, Characterization of the *tol-pal* and *cyd* region of *Escherichia coli* K-12: transcript analysis and identification of two new proteins encoded by the *cyd* operon, J. Bacteriol. 179 (1997) 2077–2080.
[21] M.R. Hemm, B.J. Paul, T.D. Schneider, G. Storz, K.E. Rudd, Small membrane proteins found by comparative genomics and ribosome binding site models, Mol. Microbiol. 70 (2008) 1487–1501.
[22] F. Fontaine, R.T. Fuchs, G. Storz, Membrane localization of small proteins in *Escherichia coli*, J. Biol. Chem. 286 (2011) 32464–32474.
[23] A. Marchler-Bauer, et al., CDD: conserved domains and protein three-dimensional structure, Nucleic Acids Res. 41 (2013) D348–D352.

[24] Y.-H. Sun, et al., The small protein CydX is required for function of cytochrome *bd* oxidase in *Brucella abortus*, Front. Cell. Infect. Microbiol. 2 (2012) 47.
[25] C.E. Vanorsdel, et al., The *Escherichia coli* CydX protein is a member of the CydAB cytochrome *bd* oxidase complex and is required for cytochrome *bd* oxidase activity, J. Bacteriol. 195 (2013) 3640–3650.
[26] M. Jin, et al., Unique organizational and functional features of the cytochrome *c* maturation system in *Shewanella oneidensis*, PLoS ONE 8 (2013) e75610.
[27] L. Wu, J. Wang, P. Tang, H. Chen, H. Gao, Genetic and molecular characterization of flagellar assembly in *Shewanella oneidensis*, PLoS ONE 6 (2011) e21479.
[28] H. Gao, et al., Physiological roles of ArcA, Crp, and EtrA and their interactive control on aerobic and anaerobic respiration in *Shewanella oneidensis*, PLoS ONE 5 (2010) e15295.
[29] S. Le Laz, A. Kpebe, M. Bauzan, S. Lignon, M. Rousset, M. Brugna, A biochemical approach to study the role of the terminal oxidases in aerobic respiration in *Shewanella oneidensis* MR-1, PLoS ONE 9 (2014) e86343.
[30] J. Yuan, B. Wei, M. Shi, H. Gao, Functional assessment of EnvZ/OmpR two-component system in *Shewanella oneidensis*, PLoS ONE 6 (2011) e23701.
[31] L. Sun, M. Jin, W. Ding, J. Yuan, J. Kelly, H. Gao, Posttranslational modification of flagellin FlaB in *Shewanella oneidensis*, J. Bacteriol. 195 (2013) 2550–2561.
[32] Q. Luo, Y. Dong, H. Chen, H. Gao, Mislocalization of Rieske protein PetA predominantly accounts for the aerobic growth defect of tat mutants in *Shewanella oneidensis*, PLoS ONE 8 (2013) e62064.
[33] Kerppola, T. K. Design and implementation of bimolecular fluorescence complementation (BiFC) assays for the visualization of protein interactions in living cells. Nat. Protocols 1 (2006) 1278-1286.
[34] L. Käll, A. Krogh, E.L.L. Sonnhammer, Advantages of combined transmembrane topology and signal peptide prediction—the Phobius web server, Nucleic Acids Res. 35 (2007) W429–W432.
[35] U. Omasits, C. Ahrens, S. Müller, B. Wollscheid, Potter: interactive protein feature visualization and integration with experimental proteomic data, Bioinformatics 30 (2013) 884–886.
[36] Y. Dong, J. Wang, H. Fu, G. Zhou, M. Shi, H. Gao, A Crp-dependent two-component system regulates nitrate and nitrite respiration in *Shewanella oneidensis*, PLoS ONE 7 (2012) e51643.
[37] M. Shi, T. Gao, L. Ju, Y. Yao, H. Gao, Effects of FlrBC on flagellar biosynthesis of *Shewanella oneidensis*, Mol Microbiol 93 (2014) 1269–1283.
[38] J. Yin, et al., Expression of *blaA* underlies unexpected ampicillin-induced cell lysis of *Shewanella oneidensis*, PLoS ONE 8 (2013) e60460.
[39] D. Schneider, T. Volkmer, M. Rögner, PetG and PetN, but not PetL, are essential subunits of the cytochrome b_6f complex from *Synechocystis* PCC 6803, Res. Microbiol. 158 (2007) 45–50.
[40] J.S. Kostecki, H. Li, R.J. Turner, M.P. DeLisa, Visualizing interactions along the *Escherichia coli* twin-arginine translocation pathway using protein fragment complementation, PLoS ONE 5 (2010) e9225.
[41] E.C. Hobbs, X. Yin, B.J. Paul, J.L. Astarita, G. Storz, Conserved small protein associates with the multidrug efflux pump AcrB and differentially affects antibiotic resistance, Proc. Natl. Acad. Sci. USA 109 (2012) 16696–16701.
[42] S. Garbis, G. Lubec, M. Fountoulakis, Limitations of current proteomics technologies, J. Chromatogr. A 1077 (2005) 1–18.
[43] M.A. Basrai, P. Hieter, J.D. Boeke, Small open reading frames: beautiful needles in the haystack, Genome Res. 7 (1997) 768–771.
[44] P.F. Cliften, et al., Surveying *Saccharomyces* genomes to identify functional elements by comparative DNA sequence analysis, Genome Res. 11 (2001) 1175–1186.
[45] M.R. Hemm, B.J. Paul, J. Miranda-Ríos, A. Zhang, N. Soltanzad, G. Storz, Small stress response proteins in *Escherichia coli*: proteins missed by classical proteomic studies, J. Bacteriol. 192 (2010) 46–58.
[46] E.C. Hobbs, J.L. Astarita, G. Storz, Small RNAs and small proteins involved in resistance to cell envelope stress and acid shock in *Escherichia coli*: analysis of a bar-coded mutant collection, J. Bacteriol. 192 (2010) 59–67.
[47] J.P. Kastenmayer, et al., Functional genomics of genes with small open reading frames (sORFs) in *S. cerevisiae*, Genome Res. 16 (2006) 365–373.
[48] F. Rappaport, J. Zhang, M.H. Vos, R.B. Gennis, V.B. Borisov, Heme–heme and heme–ligand interactions in the di-heme oxygen-reducing site of cytochrome *bd* from *Escherichia coli* revealed by nanosecond absorption spectroscopy, Biochim. Biophys. Acta 1797 (2010) 1657–1664.
[49] T. Mogi, S. Endou, S. Akimoto, M. Morimoto-Tadokoro, H. Miyoshi, Glutamates 99 and 107 in transmembrane helix III of subunit I of cytochrome *bd* are critical for binding of the heme b_{595}–*d* binuclear center and enzyme activity, Biochemistry 45 (2006) 15785–15792.
[50] V.B. Borisov, I. Belevich, D.A. Bloch, T. Mogi, M.I. Verkhovsky, Glutamate 107 in subunit I of cytochrome *bd* from *Escherichia coli* is part of a transmembrane intraprotein pathway conducting protons from the cytoplasm to the heme b_{595}/heme *d* active site, Biochemistry 47 (2008) 7907–7914.
[51] V.B. Borisov, E. Forte, P. Sarti, M. Brunori, A.A. Konstantinov, A. Giuffrè, Redox control of fast ligand dissociation from *Escherichia coli* cytochrome *bd*, Biochem. Biophys. Res. Commun. 355 (2007) 97–102.
[52] J. Zhang, P. Hellwig, J.P. Osborne, R.B. Gennis, Arginine 391 in subunit I of the cytochrome *bd* quinol oxidase from *Escherichia coli* stabilizes the reduced form of the hemes and is essential for quinol oxidase activity, J. Biol. Chem. 279 (2004) 53980–53987.
[53] Y. Matsumoto, et al., Mass spectrometric analysis of the ubiquinol-binding site in cytochrome *bd* from *Escherichia coli*, J. Biol. Chem. 281 (2006) 1905–1912.
[54] C. Brochier-Armanet, E. Talla, S. Gribaldo, The multiple evolutionary histories of dioxygen reductases: implications for the origin and evolution of aerobic respiration, Mol. Biol. Evo. 26 (2009) 285–297.
[55] J. Hoeser, S. Hong, G. Gehmann, R.B. Gennis, T. Friedrich, Subunit CydX of *Escherichia coli* cytochrome *bd* ubiquinol oxidase is essential for assembly and stability of the di-heme active site, FEBS lett. 588 (2014) 1537–1541.